Digital Object Identifier 10.1109/IMFW49589.2021.9642301

2021 IEEE MTT-S International Microwave Filter Workshop (IMFW)

Effects of Cutting Planes on Filter Performance of FDM 3D-Printed X-Band Waveguide Filters

Daniel Bruhn
Daniel Miek
Kennet Braasch
Fynn Kamrath
Chad Bartlett
Patrick Boe
Michael Höft

Suggested Citation

D. Bruhn *et al*., "Effects of Cutting Planes on Filter Performance of FDM 3D-Printed X-Band Waveguide Filters," *IEEE MTT-S International Microwave Filter Workshop (IMFW)*, 2021, pp. 236-238.

Effects of Cutting Planes on Filter Performance of FDM 3D-Printed X-Band Waveguide Filters

Daniel Bruhn*, Daniel Miek*, Kennet Braasch*, Fynn Kamrath*, Chad Bartlett*, Patrick Boe*, and Michael Höft*

* *Chair of Microwave Engineering, Institute of Electrical Engineering and Information Technology, Faculty of Engineering, Kiel University, Germany*

{stu126289, dami, keb, flk, chb, pabo, mh}@tf.uni-kiel.de

***Abstract*—In this paper, the impact of E-plane and H-plane cuts on filter performance of 3D-printed waveguide filters manufactured with fused deposition modeling (FDM) is examined. The employed manufacturing procedure consists of FDM 3D-printing and the subsequent electroplating process. A number of samples in both configurations are fabricated and surveyed. The measurement results are quantified and a comparison is conducted. Finally, the differing filter behaviors are discussed.**

***Index Terms*—Cutting planes, FDM 3D-printing, filter performance, waveguide filters, X-band.**

I. Introduction

The introduction of additive manufacturing (AM) techniques as potential production methods for waveguide filters opened up new possibilities and degrees of freedom in filter design processes (e.g. [1], [2]). Additionally, this advancement allows for rapid prototyping of filter structures, even if their final realization is attained with a different, perhaps more suitable manufacturing process [3]. Although there are various high-precision AM-techniques, the less precise fused deposition modeling (FDM) method is widely available and inexpensive while still being able to deliver useful results for prototyping applications [4], [5]. To investigate the impact of segmentation along E-plane and H-plane of the filter structure due to possible manufacturing constraints, several iterations of X-band filters in the respective configurations are realized and compared.

In Sec. II the structure and behavior of the analyzed filter is presented, whereas Sec. III discusses the manufacturing process composed of fabrication with the FDM-technique and the subsequent electroplating procedure. Finally, the various achieved filter performances are evaluated, compared and interpreted in Sec. IV and Sec. V.

II. Filter Design

To facilitate the generation of an adequately large sample size, a relatively simple third order all-pole Chebyshev filter is chosen for production (s. Fig. 1). The filter structure is realized with three rotated rectangular resonators, which are intersecting each other to achieve the necessary coupling strengths. Radii are introduced at the corners of the resonators, as unnecessary edges and deep corners complicate the metallization process described in Sec. III. The filter is designed for a return loss $RL = 20$ dB with a bandwidth $B = 0.5$ GHz at the center frequency $f_0 = 10.25$ GHz and consequently provides a fractional bandwidth of 4.88%. A corresponding 3 dB-bandwidth of $B_{3\text{dB}} = 0.81$ GHz is determined.

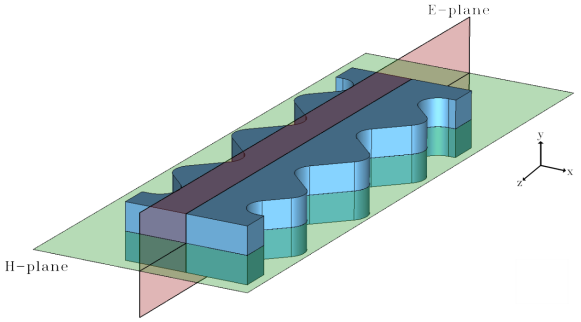

Fig. 1. Interior of the third order all-pole filter structure consisting of intersecting rectangular resonators. E-plane and H-plane are highlighted.

III. Manufacturing Process

The manufacturing process of the presented X-band filters, independent of the chosen cutting plane, is constituted by fabrication with the FDM 3D-printing method and a subsequent electroplating procedure. In preparation for production, the filter body is separated into two symmetrical halves along the E-plane or H-plane as shown in Fig. 1. The symmetrical H-plane is chosen to simplify the electroplating process (s. Sec. III-B), as this results in shallower, uniform cavities in contrast to a separation at the top or bottom of the resonators. To enable assembly after the realization, appropriate flanges are added to the structure (s. Fig. 2).

A. FDM 3D-Printing Process

The FDM-printer consists of a movable extruder and a heated building platform [3]. The used Polyactide (PLA) material is fed to the printer in form of filament, which is liquified and extruded through the nozzle onto the building

This project has received funding from the European Union's Horizon 2020 research and innovation programme under the Marie Skłodowska-Curie grant agreement 811232-H2020-MSCA-ITN-2018.

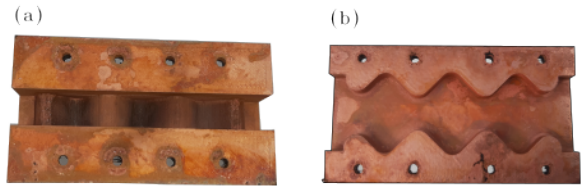

Fig. 2. (a) Realized filter half of the E-plane configuration. (b) Realized filter half of the H-plane configuration.

platform [3]. In this fashion, the filter structure is constructed layer by layer [1]. To achieve adequately smooth surfaces, a nozzle diameter of 0.4 mm and a layer height of 0.1 mm is chosen. Although the FDM 3D-printing technique enables the production of objects not achievable with more conventional subtractive fabrication methods [1], some limitations apply. Deformation of the still flexible material is prevented with the implementation of a suitable support structure during the printing process. The E-plane and H-plane configurations only require supports on the outside of the filter, as they are fabricated in x- and y-direction, respectively (s. Fig. 1). The amount of required PLA-material as well as manufacturing time is reduced by applying a honeycombed infill structure.

B. Electroplating Procedure

Since the manufactured workpiece is made up of non-conductive plastic, a conducting surface coating has to be applied to achieve the desired filter performance. For this purpose, the surface of the filter structure is cleaned and degreased. Subsequently, two layers of weakly conducting copper spray paint are applied, while minimum drying times of 12 h per coating are observed. The final, highly conductive layer is realized with the electroplating procedure. In this process, a current flow through an electrolyte solution is used to grow a copper layer on the structure. The copper atoms are released by a sacrificial anode and deposited on the workpiece, which functions as the cathode [6]. The applied current is increased step by step from 75 mA to 100 mA over the duration of the approximately 8 h lasting procedure. Initially, the workpiece is turned in the electrolyte solution in 30 min intervals to ensure an even deposition of the copper layer.

IV. Results and Evaluation

In order to gain a representative overview on the effect of cutting planes on filter performance, seven realizations in both E-plane- and H-plane configuration have been produced. The comparison of the results is based on the achieved center frequency f_0, 3 dB-bandwidth $B_{3\text{dB}}$ and the estimated unloaded quality factor Q_u [7].

A. E-plane Realizations

An example of a FDM 3D-printed and subsequently electroplated E-plane filter half is shown in Fig. 2(a). The measured S-parameters of the filters separated at the E-plane are displayed in Fig. 3, while the related comparables are collected in Tab. I. A mean 3 dB-bandwidth $\overline{B}_{E,3\text{dB}} = 0.83$ GHz at the mean center frequency $\overline{f}_{0,E} = 10.25$ GHz is determined. There is only a negligible shift of the mean center frequency, though an associated standard deviation of 60 MHz is calculated. The mean 3 dB-bandwidth is increased by approximately 20 MHz. The highest achieved quality factor is $Q_{u,E4} \approx 4500$, whereas a sample mean $\overline{Q}_{u,E} \approx 2957$ with an empirical standard deviation $\tilde{s}_{Q_u,E} \approx 1244$ is ascertained.

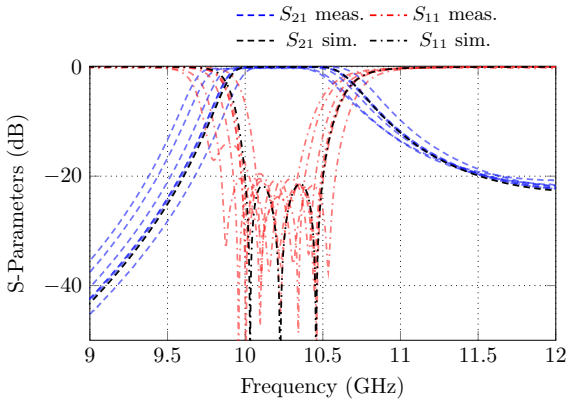

Fig. 3. Measured S-parameters of the filters in E-plane configuration.

TABLE I
Measurement results of the filters in E-plane configuration
(all frequency values in GHz)

Iter.	f_0	$B_{3\text{dB}}$	Q_u	RL/dB	Δf_0	$\Delta B_{3\text{dB}}$
E1	10.36	0.82	4200	20.94	0.11	0.01
E2	10.23	0.83	1600	20.80	-0.02	0.02
E3	10.15	0.83	1000	20.40	-0.10	0.04
E4	10.23	0.85	4500	19.53	-0.02	0.02
E5	10.28	0.83	4000	20.89	0.03	0.02
E6	10.26	0.82	2800	20.46	0.01	0.01
E7	10.22	0.84	2600	20.47	-0.03	0.03
mean	10.25	0.83	2957	20.50	0	0.02
$\tilde{s}$	0.06	0.01	1244	0.45	0.06	0.01

B. H-plane Realizations

A fabricated filter half of the H-plane configuration is depicted in Fig. 2(b). The measured S-parameters of the filters cut at the H-plane are displayed in Fig. 4 and the associated comparables are collected in Tab. II. A mean bandwidth $\overline{B}_{H,3\text{dB}} = 0.83$ GHz at the mean center frequency $\overline{f}_{0,H} = 10.25$ GHz with an empirical standard deviation of 20 MHz is determined. Accordingly, there is only a negligible mean deviation from the simulated center frequency and a mean 3 dB-bandwidth increase of approximately 20 MHz. The highest achieved Quality factor is $Q_{u,H5} \approx 1900$, whereas a sample mean $\overline{Q}_{u,H} \approx 1183$ with an empirical standard deviation $\tilde{s}_{Q_u,H} \approx 478$ is estimated.

C. Comparison

The calculated sample mean $\overline{Q}_{u,H}$ for the given sample size corresponds to only 40% of the sample mean $\overline{Q}_{u,E}$ achieved by the filters in E-plane configuration. The larger empirical standard deviation $\tilde{s}_{Q_u,E}$ of the E-plane realizations indicates more disparate measurements, but in relation to the widely

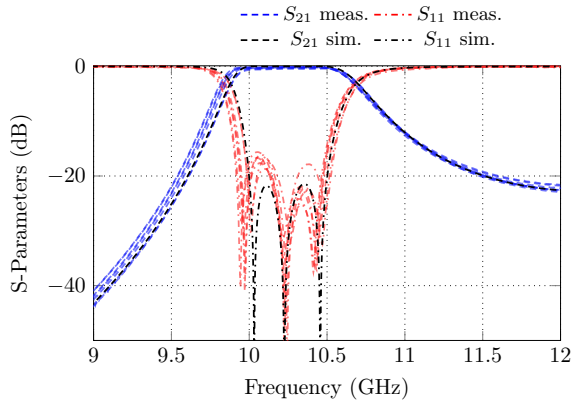

Fig. 4. Measured S-parameters of the filters in H-plane configuration.

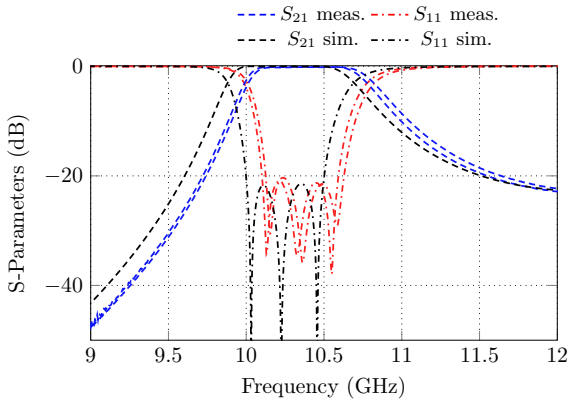

Fig. 5. Measured S-parameters of the monolithic filter realization examples.

TABLE II
MEASUREMENT RESULTS OF THE FILTERS IN H-PLANE CONFIGURATION (ALL FREQUENCY VALUES IN GHZ)

Iter.	f_0	$B_{3\text{dB}}$	Q_u	RL/dB	Δf_0	$\Delta B_{3\text{dB}}$
H1	10.28	0.81	730	16.79	0.03	0.01
H2	10.25	0.83	1300	16.57	0	0.02
H3	10.26	0.83	1100	16.15	0.01	0.02
H4	10.24	0.85	900	15.62	-0.01	0.04
H5	10.23	0.84	1900	16.71	-0.01	0.03
H6	10.24	0.82	1800	17.56	-0.02	0.01
H7	10.28	0.80	550	17.86	0.03	0.01
mean	10.25	0.83	1183	16.75	0	0.02
$\tilde{s}$	0.02	0.02	478	0.5	0.02	0.02

differing sample means, the H-plane configuration exhibits similarly consistent results. This behavior can be explained by the field distributions and resulting surface currents in the filter interior. In E-plane configuration, no significant currents flow across the contact surfaces of the two filter halves, whereas the opposite occurs in the case of the H-plane configuration. Imperfections at the edges and interfaces caused by the FDM-manufacturing procedure as well as the electroplating process result in higher contact resistances. Thus, the imperfections of the H-plane configuration have a greater influence and result in a worse filter performance in comparison to the other realization. General defects of the copper layer might still worsen the measurement results, as exemplified by the realizations E2 and E3 of the E-plane configuration. These imperfections have the potential to be more or less impactful, depending on whether critical areas are affected. Additionally, further losses and distortions might be introduced by misaligning the filter halves. Similar minimal deviations in center frequency and 3 dB-bandwidth are achieved with both filter configurations, while the results of the H-plane filters are more homogeneous in this regard. Reliably good RL-performance has been attained with E-plane configurations. The results for H-plane realizations are poorer and less consistent.

Potential issues with misaligned filter halves and losses at interfaces can be avoided by realizing a monolithic filter only consisting of a single part. 3D-printing allows for the production of the monolithic filter structure in z-direction (s. Fig. 1), but new manufacturing difficulties arise e.g. from the necessity of support structures and complication of the electroplating process. As an example, two monolithic realizations with the quality factors $Q_{u,M1} \approx 1700$ and $Q_{u,M2} \approx 2400$ are produced (s. Fig. 5). Both filters exhibit a large respective center frequency shift in comparison to the other realizations, while a higher Q_u-value than realized with any H-plane structure is determined for filter M1.

V. CONCLUSION

Overall, the described manufacturing technique consisting of FDM 3D-printing and the subsequent electroplating procedure is employable for prototyping of filters cut at E- and H-plane. At that, the best and most consistent results have been achieved with filters separated at the E-plane. On average, the filters cut at the H-plane delivered only 40% of the Q_u-values attained with the other configuration. Despite the worse performance, H-plane realizations might still be useful to estimate filter behavior.

REFERENCES

[1] C. Tomassoni, O. A. Peverini, G. Venanzoni, G. Addamo, F. Paonessa, and G. Virone, "3D printing of microwave and millimeter-wave filters: Additive manufacturing technologies applied in the development of high-performance filters with novel topologies," *IEEE Microwave Magazine*, vol. 21, no. 6, pp. 24–45, Jun. 2020.

[2] J. R. Montejo-Garai, I. O. Saracho-Pantoja, C. A. Leal-Sevillano, J. A. Ruiz-Cruz, and J. M. Rebollar, "Design of microwave waveguide devices for space and ground application implemented by additive manufacturing," in *2015 International Conference on Electromagnetics in Advanced Applications (ICEAA)*. IEEE, Sep. 2015.

[3] F. Calignano, D. Manfredi, E. P. Ambrosio, S. Biamino, M. Lombardi, E. Atzeni, A. Salmi, P. Minetola, L. Iuliano, and P. Fino, "Overview on additive manufacturing technologies," *Proceedings of the IEEE*, vol. 105, no. 4, pp. 593–612, Apr. 2017.

[4] N. S. A. Bakar, M. R. Alkahari, and H. Boejang, "Analysis on fused deposition modelling performance," *Journal of Zhejiang University-SCIENCE A*, vol. 11, no. 12, pp. 972–977, Dec. 2010.

[5] A. Gomez-Torrent, F. Teberio, A. Martinez, J. M. Percaz, I. Arnedo, I. Maestrojuan, I. Arregui, G. Crespo, T. Lopetegi, M. A. G. Laso, and J. Teniente, "A study of the additive manufacturing technology for RF/microwave components," in *2017 11th European Conference on Antennas and Propagation (EUCAP)*. IEEE, Mar. 2017.

[6] M. Albach, *Elektrotechnik*, 1st ed. Pearson, Aug. 2011.

[7] G. Macchiarella, "Extraction of unloaded Q and coupling matrix from measurements on filters with large losses," *IEEE Microwave and Wireless Components Letters*, vol. 20, no. 6, pp. 307–309, Jun. 2010.